

# FACE RECONSTRUCTION WITH STRUCTURED LIGHT

John Congote<sup>1,2</sup>, Iñigo Barandiaran<sup>1</sup>, Javier Barandiaran<sup>1</sup>, Marcos Nieto<sup>1</sup>

<sup>1</sup>Vicomtech Research Center, Donostia - San Sebastian, Spain

Oscar Ruiz<sup>2</sup>

<sup>2</sup>CAD CAM CAE Laboratory, EAFIT University, Medellín, Colombia

Keywords: 3D Reconstruction, Structured light, Gray codes, Depthmap.

Abstract: This article presents a methodology for reconstruction of 3D faces which is based on stereoscopic images of the scene using active and passive surface reconstruction. A sequence of Gray patterns is generated, which are projected onto the scene and their projection recorded by a pair of stereo cameras. The images are rectified to make coincident their epipolar planes and so to generate a stereo map of the scene. An algorithm for stereo matching is applied, whose result is a bijective mapping between subsets of the pixels of the images. A particular connected subset of the images (e.g. the face) is selected by a segmentation algorithm. The stereo mapping is applied to such a subset and enables the triangulation of the two image readings therefore rendering the  $(x, y, z)$  points of the face, which in turn allow the reconstruction of the triangular mesh of the face. Since the surface might have holes, bilateral filters are applied to have the holes filled. The algorithms are tested in real conditions and we evaluate their performance with virtual datasets. Our results show a good reconstruction of the faces and an improvement of the results of passive systems.

## 1 INTRODUCTION

### 1.1 Mathematical Context

In general, surface reconstruction from optical samples requires a function  $G$  relating pixels in an image of the scene  $A \times B$  ( $A, B \subset \mathbb{N}$ ) with points  $p \in \mathbb{R}^3$ . This function,  $G: A \times B \rightarrow \mathbb{R}^3$ , is an injection since the image only records the visible part of the scene.  $G$  is not an onto function, as there are many points  $p \in \mathbb{R}^3$  for which there is no pixel  $(i, j) \in A \times B$  in the image that records them.

Once this geometry function  $G$  is known, it is relatively simple to build a triangular mesh of the portion of the object visible in the image. Under a threshold of geometrical proximity,  $G(i, j), G(i + i, j), G(i + 1, j + 1)$  may be considered the vertices of a triangular facet of the sought surface  $M$ . Moreover, the triangles being natural neighbors to triangle  $t = [G(i, j), G(i + i, j), G(i + 1, j + 1)]$  are the ones involving pixels  $(i, j + 1), (i + 2, j + 1), (i, j - 1)$ , again, under thresholds of geometrical proximity. Stitching the different  $M$  triangular meshes originated in different views of the scene is known as zippering, and is

not in the scope of our article. Literature on the topic might be found in (Greg Turk, 1994), (Marras et al., 2010) and (Shen et al., 2004).

The discussion in this article involves two images, which may be labeled, without losing generality, as *right* and *left*,  $I_R$  and  $I_L$ . Simplifying the discussion, a color image is a mapping  $I: A \times B \rightarrow [0, 255]^3$ . For example,  $I(i, j) = (143, 23, 112)$  means that the color registered in the pixel  $(i, j)$  of  $I$  corresponds to Red=143, Green=23 and Blue=112. A grey scale image has the form  $I(i, j) = (k, k, k)$  due to the fact that in it the Red, Green and Blue graduations are identical ( $k \in [0, 255]$ ).

Let  $S_L$  and  $S_R$  be the coordinate systems associated to images Left and Right, respectively. In the general configuration of the set-up,  $S_L$  and  $S_R$  such that (1) the  $Z$  axis of the coordinate system is normal to the capture plane of the image, and (2) the two cameras point to a common point  $p \in \mathbb{R}^3$ . In this article we assume that the images are *rectified*. This means, both of them have been rotated inside their own  $X - Y$  plane (i.e. rotation around the  $Z$  axis of the image) in such a manner that the epipolar plane of the set-up is seen as the plane  $y = E_c$  in both images. That means,



Figure 1: Results of the algorithm with the virtual dataset. Smooth surfaces are obtained with wider baselines.

the epipolar plane is seen as the same horizontal line in both images. We call the rectified images  $I_R$  and  $I_L$  and their rectified and their rectified coordinate systems  $S_L$  and  $S_R$ , respectively.

Let us consider a point  $p \in \mathbb{R}^3$  recorded in both images  $I_R$  and  $I_L$ . Because the previous assumptions we have that  $G_L(i, j) = p$  and  $G_R(i, k) = p$ . This means, the point  $p$  appears in the same row  $i$  of pixels in both images. The value  $|k - j|$  is an offset that only occurs in the same pixel row of both images. Since we know that pixels  $(i, j)$  in image  $I_L$  and  $(i, k) = p$  in image  $I_R$  record the same point  $p \in \mathbb{R}^3$ , the point  $p$  can be recovered by a usual triangulation procedure.

## 1.2 Informal Context

Human face reconstruction is a common problem in computer vision and computer graphics (Stylianou and Lanitis, 2009), where one possible objective is the generation and animation of a virtual model of it. The face is one of the most important identification regions of the human body, presenting commensurate technical challenges (Zhao et al., 2003). A correct reconstruction of human faces is a precondition to both augmented reality and face recognition.

3D surface reconstruction may be achieved by both passive and active methods. passive ones do not change the environment in the process of reconstruction. Even though passive methods obtain very good results, their setups are very expensive because they required a very high resolution required for obtaining reasonable results (Beeler et al., 2010).

Active systems modify or adapt the environment during the capture process. Our active system uses the projection of a light pattern (i.e. *structured light*), which is widely used for face surface reconstruction. In structured light systems any change on the setup requires new algorithms for face (surface) reconstruction.

The 3D surface reconstruction system implemented and informed in this article is part of a system used for full body reconstruction with visual hull algorithm (Haro and Pardís, 2010). Our setup applied to a face-body model produces a triangular mesh with high detail in the face region and low detail in the rest of the body. The reason for this differential resolution

is that, while for the face region one requires high frequency details (e.g. texture of the skin), for the rest of the body such details are not required in our applications.

This article presents a system for face reconstruction which articulates non-proprietary hardware and our own software to obtain geometrical information from two images (possibly originated in 3D video - conference set ups). Our system also recovers the 3D geometry from the body region, although intentionally using lower resolution for neighborhoods other than the face.

This paper, Section 2 reviews previous works in face reconstruction. Section 3 presents the methodology implemented, including generation of the light patterns, capture, segmentation and reconstruction. Section 4 discusses the hardware set-up for the experiment and its configuration. Section 5 presents the results of the 3D surface reconstruction set-up and algorithms, and evaluates the reconstructed models against with real data. Section 6 concludes the work and proposes the future actions in this domain.

## 2 RELATED WORK

Face reconstruction is a widely studied topic. (Pighin and Lewis, 2005) presents a tutorial on face reconstruction, describing different problems and approaches from an artistic point of view, looking for a correct representation of the face and its expressions in multi-media. (Stylianou and Lanitis, 2009) presents a survey of 3D face reconstruction methods, classifying them in three different categories: *single image*, *stereo images* and *videos*.

passive systems are commonly used for face reconstruction. One of the advantages of these systems is their non interaction with the environment, allowing to capture the geometry without interfering with other systems. (Onofrio et al., 2005) uses a system with four calibrated cameras applying a multi - view algorithm. A stochastic model is generated for the identification of the geometry, by minimizing a cost function. (Leclercq et al., 2005) compares different stereo algorithms for face reconstruction, and proposes an appropriate geometrical configuration of cameras to obtain accurate results. (Alexander et al., 2009) presents a complex setup to a high resolution face reconstruction system. The methodology is based on an iterative reconstruction of the face by incrementing the size of the image and the number of stereo pairs used in each step. (Beeler et al., 2010) extends the approach proposed in (Alexander et al., 2009) by adding a post-processing step that modifies the geometry of the face

by using a texture, assuming that small dark regions of the face represent small hollows. This approach obtaining a more rich geometry.

Structured light for 3D reconstruction have been study for several years. The information obtained with this kind of systems is already being used as ground truth data for the evaluation of pasive reconstruction systems, such as stereo algorithms (Scharstein and Szeliski, 2003). An extensive survey of structured light 3D reconstruction approaches can be found in (Salvi et al., 2010), where a classification of different coding techniques are presented and evaluated. They identify the best coding approach for each one of the possible scenario configurations such as static o moving scenarios or if the light conditions are controlled.

Real time capture of facial expressions is also an important feature in some systems. Several problems have to be addressed to accomplish this objective. One of these problems is the difficulty of projecting several patterns for a reconstruction in non static scenes where small moves generate artifacts in the reconstructions, so other patterns have been employed which uses color models as (Tsalakanidou et al., 2005) which allows a denser codification of the pattern, also single frame reconstruction with 2D coding is possible(Chen et al., 2008). Another problem is hardware calibration to obtain several frames per second with a correct synchronization process between the projector and the cameras. An accepted synchronization approach can be found in (Zhang et al., 2006). Finally, for a correct pattern codification of time variant patterns, a motion compensation should be implemented. This issue is especially critical for face reconstruction systems, where the person being reconstructed could move in a involuntary way,during acquisition (Weise et al., 2007)

### 3 METHODOLOGY

Our algorithm of face reconstruction uses a set of stereo images captured at the same moment when a pattern is projected into the face. The images are captured in a setup previously calibrated. We assume that the object does not move between the different captures and the face is assumed to be a smooth surface without hair or beard and without highlight reflections. The result is a mesh of triangles correctly positionated in the space which represent the face region.

#### 3.1 Stereo Calibration

Stereo calibration refers to the task of finding the relative pose between the cameras of a stereo pair. The objective is to feed subsequent stereo rectification processes that align the images such that the epipolar lines are horizontal and thus matching algorithms for 3D reconstruction can be implemented as one-dimensional searches.

Typically, stereo calibration is carried out by means of finding a number of point-correspondences between the images of the pair and retrieving the fundamental matrix. Let  $\mathbf{x}$  be the image of a 3D point in the left image, and  $\mathbf{x}'$  the image of the same point in the right image. The fundamental matrix restricts the position of  $\mathbf{x}'$  to the epipolar line associated to  $\mathbf{x}$ , such that  $\mathbf{x}'^T F \mathbf{x} = 0$ . It has been shown (Hartley and Zisserman, 2004), that the knowledge of the fundamental matrix can be used to retrieve the projection matrices of the two cameras of the pair, up to a projective ambiguity that can be solved with known restrictions of the camera.

Besides, images captured by real cameras show some tangential and radial distortion, which can be corrected applying the following functions:

$$u = p_x + (u - p_x)(1 + k_1 r + k_2 r^2 + k_3 r^3 + \dots)$$

$$v = p_y + (v - p_y)(1 + k_1 r + k_2 r^2 + k_3 r^3 + \dots)$$

where  $r^2 = (u - p_x)^2 + (v - p_y)^2$  and  $k_1, k_2, k_3, \dots$  are the coefficients of the Taylor expansion of an arbitrary radial displacement function  $L(r)$ .

Parameter identification of the camera stereo pair is extracted from the calibration information of the full body reconstruction setup; which is further explained in (Ronda et al., 2008). For our purposes we select the camera pair which are focused to the face region of the body, and we follow a 3D stereo reconstruction process with them.

#### 3.2 Pattern Generation

Pattern generation refers to the task of creating of a set of synthetic binary images to be projected as structured light in the scene. The objetive is to identify the coordinates of the projected pattern in the image scene and thus allowing a point matching algorithm to become independent of the color in the captured scene.

The used patterns are represented as a matrix of boolean values. Let  $P$  be a matrix of  $M$  columns and  $N$  rows thus  $P = \{P_{m,n} \in \{0, 1\}\}$  with  $0 < m < M$  and  $0 < n < N$ . Let  $C$  be a matrix of the same dimensions of  $P$  thus  $C = \{C_{m,n} \in (0, M) \subseteq \mathbb{N}\}$ . The restriction of

---

**Algorithm 1:** Gray function to convert from binary to gray code.

---

**Input:**  $bin$   
**Output:**  $gray$   
**return**  $bin^{(bin/2)}$

---



---

**Algorithm 2:** Gray function to convert from Gray code to binary.

---

**Input:**  $gray$   
**Output:**  $bin, nPat$   
 $ish, ans, idiv \in \mathbb{N}$   
 $ish \leftarrow 1$   
 $ans \leftarrow gray$   
**while** 1 **do**  
    $idiv \leftarrow \frac{ans}{ish}$   
    $ans \leftarrow ans \oplus idiv$   
   **if**  $idiv \leq 1 \vee ish = 32$  **then**  
      **return**  $ans$   
   **end**  
    $ish \leftarrow ish \times 2$   
**end**

---

the number of values in the matrix  $C$  is the same that the number of columns allows the correct identification of the column in the images. Let  $g$  be a function such as  $g: \mathbb{N} \rightarrow \mathbb{N}$  which is bijective and transforms the numbers from binary representation to Gray representation as described in algorithm 1, the inverse Gray function  $g^{-1}$  is described in algorithm 2. The number of images to be projected depends of the number of columns of the matrix  $C$ , so  $nPat = \lceil \log_2 M \rceil$

The  $nPat$  patterns represented by the matrix  $P$  are generated as follows:

$$P_{j,k}^i = g(j) \bullet 2^i$$

where  $0 < i < nPat$  represent the number of the pattern,  $j, k$  the coordinates in the matrix  $P$ . The pattern structure can be depicted as a sequence of columns as can be visualized in the figure 2. The nature of this kind of patterns is 1D because the calibration setup already give us an epipolar constrain of the images. Therefore it is not necessary to use of 2D patterns in this case.

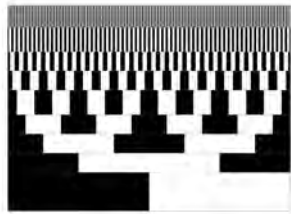


Figure 2: Gray code.

### 3.3 Pattern Recognition

Pattern recognition refers to the task of creating a pair of images which maps the position of the projected patterns  $P$  in the set of stereo pair of images. The objective is the identification of the projected pattern in the set of images, and calculate the value of the matrix  $C$  for each pixel. This matrix allow the point matching algorithm to become unambiguous since each point in the maps is labeled uniquely in each epipolar line.

Let  $s = L, R$  be matrices of  $W$  columns and  $H$  rows, thus  $L = \{L_{w,h} \in (0, 255)\}$  with  $0 < w < W$  and  $0 < h < H$ . The matrices  $L$  and  $R$  represent the information of the stereo pair cameras in grayscale. Let  $O = \{O_{w,h} \in (0, M)\}$  be the decode maps  $OL, OR$ . Let  $t: (0, 255) \rightarrow \{0, 1\}$  be a threshold function which binarizes the images  $L$  and  $R$ . The threshold value could be calculated with the Otsu algorithm as explained in (Kramer et al., 2009) or by means of calculating the albedo of the images with the process described in (Scharstein and Szeliski, 2003) where each pattern is projected two times, each one with the original version and their negative.

$$O_{m,n}^s = g^{-1} \left( \bigvee_i (s_{m,n}^i \cdot 2^i) \right)$$

As shown in figure 3 the set of  $L$  and  $R$  images are binarized. Stereo reconstruction images are combined, and a unique map  $OL$  and  $OR$  is processed. The maps should be rectified as shown in figure 4: this rectification process is possible because the camera information is already known as explained in section 3.1.

### 3.4 Stereo Reconstruction

Stereo reconstruction task calculates the point correspondence between two images. The objective is to calculate the 3D point coordinates of each pixel in the stereo images. The previous steps of the algorithm such as the stereo calibration assures the epipolar constrain. Pattern generation process gives the color independence of the images. Pattern recognition maps the set of images into a map without ambiguities. For dense depthmap calculation we used a simple box filter algorithm, based on sum of square differences  $SSD$  and a Winner Takes All  $WTA$  for pixel selection (Scharstein and Szeliski, 2002).

Let  $D$  be a matrix of  $W$  columns and  $H$  rows, thus  $D = \{D_{w,h} \in \mathbb{N}\}$ . where  $D$  describes the pixel difference between the same point in the image  $L$  and  $R$ . The identification of the correct disparity the following function is applied.

$$D_{m,n} = \text{minarg}_l (SSD(OL, OR, m, n, l))$$

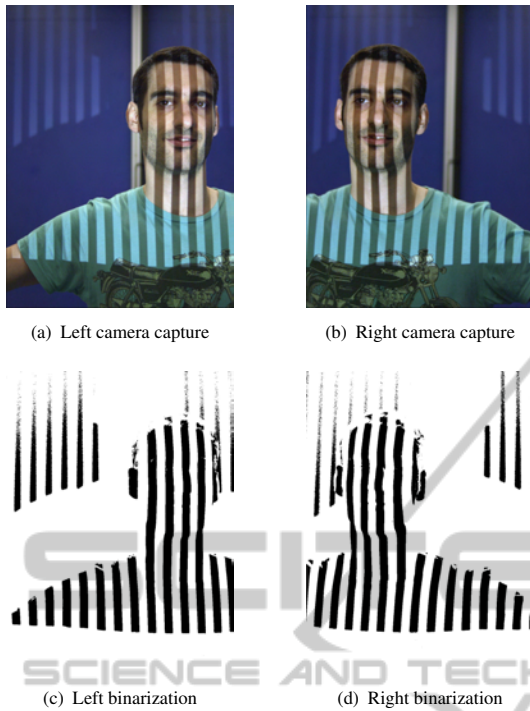


Figure 3: Stereo images captured from the cameras and their result of the threshold function.

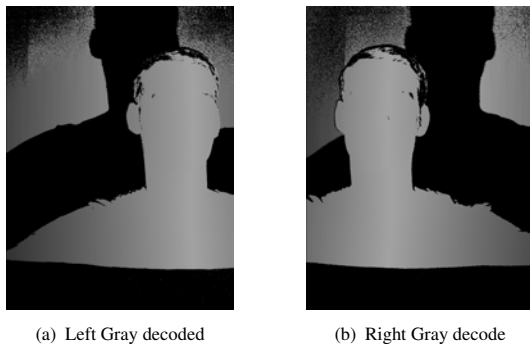


Figure 4:  $O$  maps of the images, the Gray value in each pixel represents the value of the  $C$  matrix in the stereo images.

$$SSD(L, R, m, n, l) = \sum_{e=m-b}^{m+b} \sum_{f=n-b}^{n+b} (L_{e,f} - R_{e,f+l})^2$$

The figure 5 shows the result of the disparity maps  $DL$  and  $DR$ . The identification of wrong matched points is carried out by applying process such as *cross checking* and *joint bilateral filter*. It is assumed that the biggest connected region represents the face, then a max blob algorithm is applied to filter regions outside the face. The mesh is generated by joining adjacent pixels in the image with their 3D coordinates. The topology of the mesh is correct since the difference between the coordinates of adjacent pixels are small.

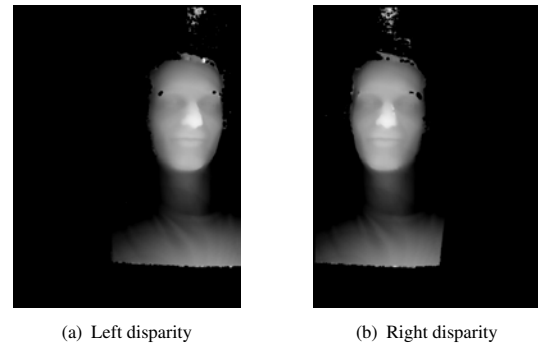


Figure 5: Stereo reconstruction of the face, the disparity images for the  $L$  and  $R$ .

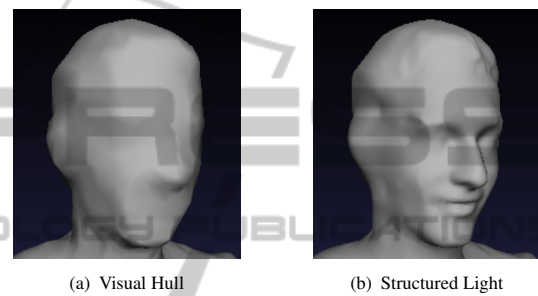


Figure 6: 3D face reconstruction.

## 4 SETUP CONFIGURATION

As our algorithm is part of a bigger chain of process where a full body reconstruction process is done. We tried to maintain the same setup for our algorithm, even we tried to use a pasive system for face reconstruction, the resolution obtained were insufficient to fulfill our needs. Then, we put a stereo camera setup with a projector in the middle of the cameras. We identified that a small distance between the cameras does not give enough information for recovering 3D positions accurately. In opposite, a wide baseline between cameras generates occlusion regions, although projection information is used for hole filling in post processing step.

The cameras used where tested with different resolutions, 1024x768, 1240x960 and 1600x1200. Finally, the resolution was set to 1240x960. Also, the projector were defined at a resolution of 800x600 because an increase of resolution generates very high frequency patterns, that are very difficult to identify accurately at that resolution. We found that a minimum width of 4 pixels for each column of the pattern is necessary for a correct identification.

Different kind of binary patterns were used. Gray pattern generates the best results. Using binary or go-

lay patterns shows in some aspects impossible to generate a workable results. In this way, we didn't consider these methods for the final version, and used only Gray codes. The binarization of the images present one of the biggest problems of the structured light setup. We used the Otsu method but it exhibits some problems, such as high sensitivity to areas of specular reflection. We finally choose the projection of the negative images with good results and a threshold  $t$  with a value of the half of the range of the gray image.

## 5 RESULTS

The evaluation of the algorithm presents several problems since the groundtruth information it is not available. However, we implemented a virtual environment which resembles a real setup. This approach allowed us to test our method and validate our results. We use Blender software for the generation of the setup and the identification of the groundtruth data, as shown in figure 8. The groundtruth was defined as a normalized depthmap with values between 0 and 255 using all the possible values in the image format as shown in the figure 7.

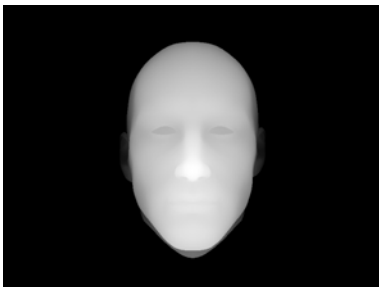


Figure 7: Ground truth depthmap image of a face.

Different camera positions were tested in our virtual setup, for the identification of the best baseline distance. The results obtained with the algorithm are shown in the figure 8. and the position of the cameras are shown in the figure 9.

The groundtruth information and the results of the algorithm show a difference in scale, but not in position. We measured the difference of the results and the groundtruth with a image correlation algorithm. The correlation gives us a value between the range of 0 and 1 where 0 is a bad results and 1 is the groundtruth. The table 1 presents the correlation values obtained for different camera position, and the figure 1 shows the 3D mesh generated.

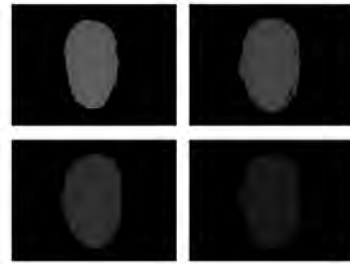


Figure 8: Result from the different cameras in the virtual setup.



Figure 9: Camera positions for virtual framework.

Table 1: Correlation Results.

Baseline distance	Value
1	0.904372
2	0.938449
3	0.958089
4	0.974051

## 6 CONCLUSIONS AND FUTURE WORK

We present a methodology for face reconstruction in a mixed environment of active-passive setup. Structured light shows a quality improvement against the results obtained with passive setups. Time multiplexing codification has the problem of motion between the captured images generating a waving effect in the reconstructions. Even robust algorithms of point matching for dense depthmaps were tested there were no real improvement in the results. We will try with color or 2D patterns which only requires one exposition that present a better approach for the reconstruction of faces since the motion problem is not present.

## ACKNOWLEDGEMENTS

This work has been partially supported by the Spanish

administration agency CDTI, under project CENIT-VISION 2007-1007. CAD/CAM/CAE Laboratory at EAFIT University and the Colombian Council for Science and Technology – COLCIENCIAS –.

## REFERENCES

- Alexander, O., Rogers, M., Lambeth, W., Chiang, M., and Debevec, P. (2009). The digital emily project: photoreal facial modeling and animation. In *ACM SIGGRAPH 2009 Courses*, SIGGRAPH '09, pages 12:1–12:15, New York, NY, USA. ACM.
- Beeler, T., Bickel, B., Beardsley, P., Sumner, B., and Gross, M. (2010). High-quality single-shot capture of facial geometry. *ACM Trans. on Graphics (Proc. SIGGRAPH)*, 29(3).
- Chen, S., Li, Y., and Zhang, J. (2008). Vision processing for realtime 3-D data acquisition based on coded structured light. *Image Processing, IEEE Transactions on*, 17(2):167–176.
- Greg Turk, M. L. (1994). Zippered polygon meshes from range images. In *ACM SIGGRAPH. Computer Graphics Proceedings, Annual Conference Series*, pages 311–318.
- Haro, G. and Pardís, M. (2010). Shape from incomplete silhouettes based on the reprojection error. *Image Vision Comput.*, 28:1354–1368.
- Hartley, R. I. and Zisserman, A. (2004). *Multiple view geometry in computer vision*. Cambridge University Press.
- Kramer, P., Boto, F., Wald, D., Bessy, F., Paloc, C., Callo, C., Letamendia, A., Ibarbia, I., Holgado, O., and Virto, J. (2009). Comparison of segmentation algorithms for the zebrafish heart in fluorescent microscopy images. In Bebis, G., Boyle, R., Parvin, B., Koracin, D., Kuno, Y., Wang, J., Pajarola, R., Lindstrom, P., Hinkenjann, A., Encarnacao, M. L., Silva, C. T., and Coming, D., editors, *Advances in Visual Computing*, Lecture Notes in Computer Science (LNCS), pages 1041–1050, Las Vegas, Nevada, USA. Springer.
- Leclercq, P., Liu, J., Woodward, A., and Delmas, P. (2005). Which stereo matching algorithm for accurate 3d face creation. In Klette, R. and Zunic, J., editors, *Combinatorial Image Analysis*, volume 3322 of *Lecture Notes in Computer Science*, pages 690–704. Springer Berlin - Heidelberg. 10.1007/978-3-540-30503-3\_53.
- Marras, S., Ganovelli, F., Cignoni, P., Scateni, R., and Scopigno, R. (2010). Controlled and adaptive mesh zippering. In *GRAPP - International Conference in Computer Graphics Theory and Applications*.
- Onofrio, D., Tubaro, S., Rama, A., and Tarres, F. (2005). 3D Face Reconstruction with a four camera acquisition system. In *Int'l Workshop on Very Low Bit-Rate Video Coding*.
- Pighin, F. and Lewis, J. P. (2005). Introduction. In *ACM SIGGRAPH 2005 Courses*, SIGGRAPH '05, New York, NY, USA. ACM.
- Ronda, J. I., Valdés, A., and Gallego, G. (2008). Line geometry and camera autocalibration. *J. Math. Imaging Vis.*, 32:193–214.
- Salvi, J., Fernandez, S., Pribanic, T., and Llado, X. (2010). A state of the art in structured light patterns for surface profilometry. *Pattern Recognition*, 43(8):2666 – 2680.
- Scharstein, D. and Szeliski, R. (2002). A taxonomy and evaluation of dense two-frame stereo correspondence algorithms. *Int. J. Comput. Vision*, 47(1-3):7–42.
- Scharstein, D. and Szeliski, R. (2003). High-accuracy stereo depth maps using structured light. In *Computer Vision and Pattern Recognition, 2003. Proceedings. 2003 IEEE Computer Society Conference on*, volume 1, pages I–195 – I–202 vol.1.
- Shen, C., O'Brien, J., and Shewchuk, J. (2004). Interpolating and approximating implicit surfaces from polygon soup. In *ACM Transactions on Graphics*, pages 896–904. ACM Press.
- Stylianou, G. and Lanitis, A. (2009). Image based 3d face reconstruction: A survey. *International Journal of Image and Graphics*, 9(2):217–250.
- Tsalakanidou, F., Forster, F., Malassiotis, S., and Strintzis, M. G. (2005). Real-time acquisition of depth and color images using structured light and its application to 3d face recognition. *Real-Time Imaging*, 11(5-6):358 – 369. Special Issue on Multi-Dimensional Image Processing.
- Weise, T., Leibe, B., and Gool, L. V. (2007). Fast 3d scanning with automatic motion compensation. In *IEEE Conference on Computer Vision and Pattern Recognition (CVPR'07)*.
- Zhang, S., Royer, D., and Yau, S.-T. (2006). High-resolution, real-time-geometry video acquisition. In *ACM SIGGRAPH 2006 Sketches*, SIGGRAPH '06, New York, NY, USA. ACM.
- Zhao, W., Chellappa, R., Phillips, P. J., and Rosenfeld, A. (2003). Face recognition: A literature survey. *ACM Comput. Surv.*, 35:399–458.